Journal of Medical Ultrasonics
https://doi.org/10.1007/s10396-024-01475-3

REVIEW ARTICLE–GASTROENTEROLOGY

Hyperechogenicity and histopathological features of focal liver lesions

Kumiko Okino[1] · Satoshi Wakasugi[2] · Shin Ichihara[3]

Received: 18 January 2024 / Accepted: 23 May 2024

Abstract
The identification and accurate diagnosis of focal liver lesions are important in modern medicine, where diagnostic radiology plays an essential role. This review aimed to examine the hyperechogenicity and histopathological features of focal liver lesions. Hyperechogenic liver lesions can be either benign or malignant. Evidence shows that hyperechogenicity is caused by factors such as fat deposition, sinusoidal dilation, peliotic changes, and pseudoglandular patterns. Fat deposition is a common cause of increased echogenicity in hepatocellular carcinoma (HCC). Meanwhile, sinusoidal dilation and peliotic changes are more frequently observed in larger HCC nodules. Pseudoglandular patterns, characterized by the reflection of ultrasound waves at the walls of numerous acini, are associated with hyperechogenicity in well-to-moderately differentiated HCCs. Moreover, this review comprehensively examined the histological features that may cause hyperechogenic internal echoes in not only HCCs but also localized liver lesions (metastases of adenocarcinoma and neuroendocrine neoplasm, intrahepatic cholangiocarcinoma, cavernous hemangioma, focal nodular hyperplasia, and angiomyolipoma). To make an accurate diagnosis and provide appropriate management, it is important to understand the histopathological basis for hyperechogenicity in focal liver lesions. By maximizing the accuracy of imaging studies and enhancing the radiology–pathology correlation, unnecessary biopsies can be avoided, thereby reducing potential complications and mortality. This review can help facilitate the effective management of patients with focal liver lesions, thereby resulting in timely and appropriate treatment decision-making.

Keywords Fatty change · Hyperechogenic hepatic lesion · Pseudoglandular pattern · Peliotic change · Sinusoidal dilation

Introduction

The detection of asymptomatic focal liver lesions is increasing because of the use of diagnostic radiology, which plays an important tool in modern medicine. Focal liver lesions are commonly benign. However, malignancy must be ruled out, which is a diagnostic challenge [1]. Early identification of premalignant and malignant focal liver lesions and provision of appropriate treatments, such as curative resection and ablation, are essential. Histopathological examination, which is an invasive procedure that removes a piece of tumor tissue, is the gold standard for cancer diagnosis. However, the role of tumor biopsy in hepatocellular carcinoma (HCC) slightly differs from that in other types of cancers. Moreover, imaging plays an important role in HCC management [2, 3]. The specificity of imaging studies for HCC diagnosis is approximately 100%. Therefore, HCC is among the few malignancies for which management can be determined based on imaging alone [4, 5]. Maximizing imaging accuracy in the context of focal liver lesions including HCC can prevent unnecessary biopsies. This may result in post-procedural complication rates of up to 6.4% and mortality rates of up to 0.1% [6].

Advances in ultrasonography (US) technology including tissue harmonics imaging, compound imaging, and speckle reduction imaging have resulted in better image quality and enhanced resolution. US has become a well-established clinical imaging technique as it can provide real-time, quantitative, anatomical and physiological information about the

✉ Shin Ichihara
trampolineboy@mbn.nifty.com

[1] Department of Clinical Laboratory Medicine, School of Medical Technology, Health Sciences University of Hokkaido, Sapporo, Japan

[2] Department of Internal Medicine, Kanto Central Hospital of the Mutual Aid Association of Public School Teachers, Tokyo, Japan

[3] Department of Surgical Pathology, Sapporo Kosei General Hospital, Sapporo, Japan

Published online: 03 July 2024

human body. The current US imaging modalities include grayscale B-mode imaging for assessing tissue morphology and echogenicity, color/power Doppler imaging for detecting and characterizing blood flow signals, elastography for examining tissue stiffness, and contrast-enhanced imaging for allowing better visualization of tumors and their vasculature. To some degree, all these techniques can provide diagnostic information on the malignancy or benignity of liver lesions [7]. Notably, US images basically reflect the pathological characteristics of focal liver lesions [8, 9].

Both benign and malignant hyperechogenic liver lesions can arise from several entities. Liver hemangioma is the most common type of benign tumor, and it typically appears as a well-defined hyperechoic lesion or hypoechoic mass with a hyperechoic periphery [10–14]. Focal nodular hyperplasia (FNH) is the second most common benign liver tumor and is occasionally hyperechoic. However, B-mode findings alone do not often reveal a typical central scar, and specific findings cannot be obtained [15]. Moreover, hepatocellular adenoma, HCC, and liver metastasis may appear as hyperechoic because of fat abundance, necrosis, or other factors [8, 16]. Consequently, hyperechogenic liver lesions encompass a wide range of conditions that are occasionally encountered during abdominal US. Further, in patients with atypical imaging characteristics of focal liver lesions, some hyperechoic lesions can be diagnosed as an unexpected pathology, thereby making the radiology–pathology correlation challenging. Even at present, a comprehensive understanding of the pathology of these lesions and their correlated imaging characteristics has become increasingly important for the accurate diagnosis and proper management of related conditions. This review aimed to assess the pathological features of various hyperechoic liver lesions and provide comprehensive knowledge on differential diagnosis.

Hyperechogenicity and pathological features of liver lesions

When US waves travel through soft tissues, a relatively small proportion of sound waves are reflected due to the minimal difference in density within the tissue. However, US waves can be reflected at the surfaces between tissues of different densities. A higher density equates to a greater impedance. If the density of a tissue increases, more US waves are reflected. In addition, human tissues comprise irregular structures. Thus, sound waves are always reflected at a slightly altered angle. Meanwhile, some waves are reflected during passage through human tissues, and reflections within the irregular structures of the tissue are more scattered.

B-mode US imaging uses a gray scale to depict the strength of the returning sound, with stronger signals being hyperechoic (white). Therefore, hyperechogenicity can be explained by mixing materials with different acoustic impedances in a single unit volume. Hyperechoic liver lesions can be detected on US due to the increased reflection of US waves caused by factors including fatty deposits, sinusoidal dilation, peliotic changes, pseudoglandular patterns, capillary vessels, fibrous septum/capsule, and hemorrhage/necrosis.

Hyperechoic liver lesions

Early hepatocellular carcinoma/hepatocellular adenoma

HCCs can vary based on the patterns of their internal echoes, with hyperechoic, hypoechoic, and mosaic patterns present in 12–38%, 23–54%, and 17–38% of cases, respectively [17]. The echo levels can vary with tumor size, with HCCs measuring < 10 mm being almost hypoechoic or isoechoic. The number of lesions with such low-level echoes increases with cell density. The two models of hepatocarcinogenesis are *de novo* carcinogenesis and stepwise development from low-grade dysplastic nodules to classical HCCs [9, 18]. The internal echoes can change during stepwise carcinogenesis [17]. During the development of early HCC, hypoxia can alter the metabolic status of tumor cells and lead to intracytoplasmic lipid accumulation [19]. Further, the blood supply changes within the nodules as hepatocarcinogenesis progresses [9, 18, 20]. Portal tracts decrease while abnormal unpaired arteries develop. The intranodular vasculature changes with increasing malignancy. Further, the supply shifts from the portal to arterial blood, eventually supplying only arterial blood to classical HCCs [9] (Fig. 1).

Fatty changes are most frequently observed (36.4%) in tumors with a diameter of 10–15 mm during tumor growth as multistep hepatocarcinogenesis. Moreover, the internal echoes of these HCCs are hyperechoic. This histological variation can explain several nodule-in-nodule appearances, which are mixed hyperechoic areas within hypoechoic lesions [21] and have been well evaluated for the development and progression of early HCC. On the contrary, the blight loop pattern is observed when early HCC with fat deposits loses its fat deposits as it progresses to advanced HCC, resulting in hypoechoic areas intermingled within a highly echogenic lesion [22, 23] (Fig. 2).

The hyperechogenicity of HCC can be caused by various factors other than lipid deposition. Sinusoidal or sinusoidal-like vasculature dilatation may result in hyperechogenicity in HCC. For HCC nodules larger than 3–4 cm, the dilation of the sinusoidal vascular spaces may be a more frequent cause of hyperechogenicity than fat deposition [23]. An altered blood flow in chronic hepatitis and in tumors with unpaired arteries, such as HCC, can directly affect the sinusoidal lumen due to arterial pressure. Damaged liver and common HCC can adapt to a high-pressure environment via the

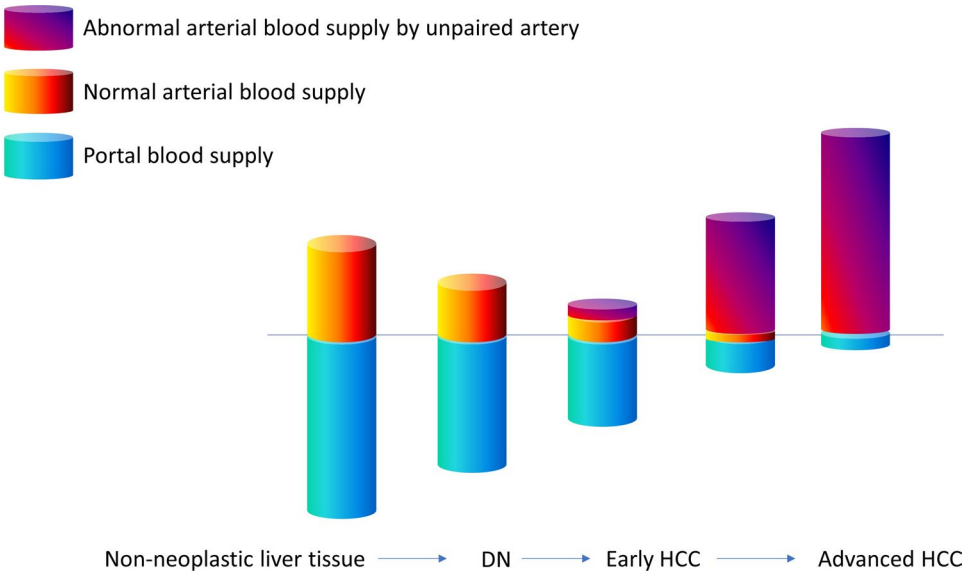

Fig. 1 As hepatocarcinogenesis progresses from a dysplastic nodule to hepatocellular carcinoma, the intranodular blood supply undergoes changes

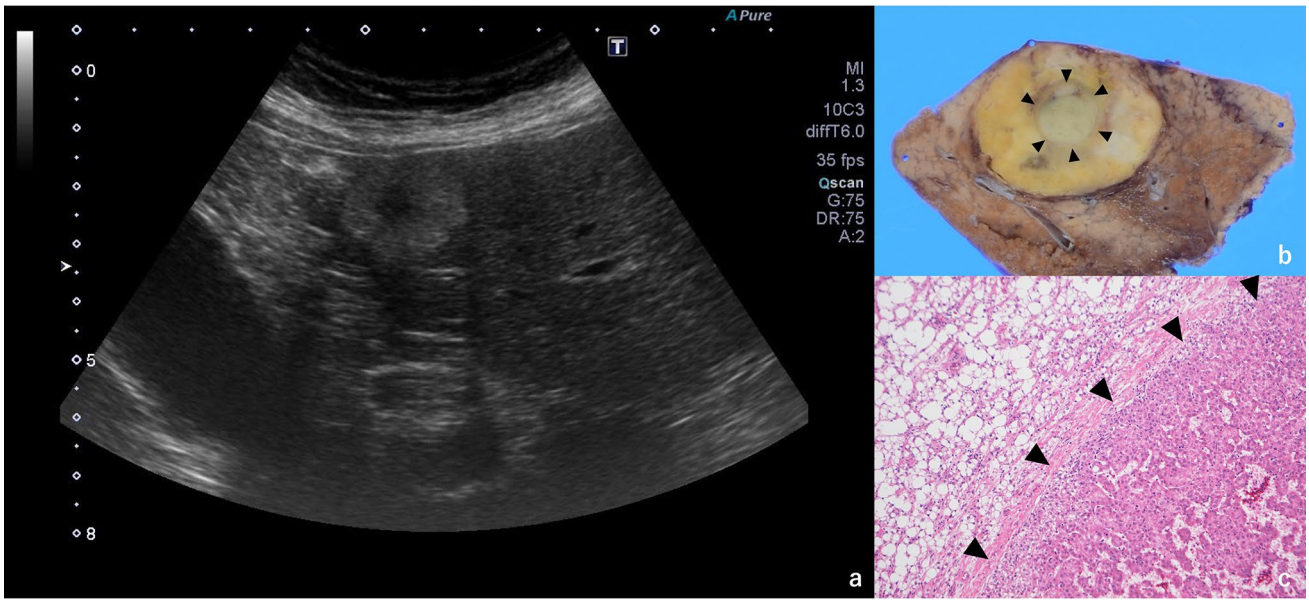

Fig. 2 Hepatocellular carcinoma with fat deposition. A nodule-in-nodule case with a bright loop pattern, displaying hyperechogenicity on the outer layer and low echogenicity on the inner layer, is observed (**a**). Gross examination revealed yellowish margins of the lesion (**b**) with histological evidence of fat deposition after staining with hematoxylin and eosin (**c**). Conversely, the interior part was macroscopic brownish. Further, microscopic examination revealed fat deposition loss due to multistep carcinogenesis (arrowhead)

capillarization of sinusoids [24]. However, in some HCCs or other tumors, the sinusoid and sinusoidal-like lumen are not sufficiently capillarized, resulting in dilation of sinusoidal lumens that cannot accommodate arterial pressure. Combining tumor cells or hepatocytes with dilated sinusoidal lumens and internal blood can create materials with different acoustic impedances, leading to a relatively hyperechogenic appearance.

In 1983, Tanaka et al. showed the presence of hyperechogenicity caused by sinusoidal dilation [16]. Fujimoto et al. focused on peliotic changes with blood retention in the dilated sinusoidal lumen [23]. Further, the mechanism of peliotic changes in HCC could be explained by endothelial damage owing to sinusoidal dilation after an increase in intratumoral pressure. Such peliotic changes include not only intratumoral bleeding but also a phenomenon caused by the restructuring of intratumoral blood vessels due to molecular biological changes such as angiopoietin-2 [25]. Notably, normal and nonneoplastic livers often exhibit peliotic change (peliosis hepatis), which is generally hypoechoic

but can also be hyperechoic or complex and often mimics a localized tumor [26].

Figure 3 shows an example of a self-experiment that can provide a better understanding of the concept. Cases of marked sinusoidal dilatation within HCC are often referred to as peliotic HCC because of the resulting relative hyperechogenicity [23, 27].

Notably, the peliotic changes causing high echoes are not always clear at the macroscopic level, and they require histopathological analysis. We had a case of HCC at our institution where most lesions appeared hyperechogenic (Fig. 4). The typical dark-colored blood spots, also known as peliotic cavities, were not prominent on gross examination. Nevertheless, microscopic examination revealed a relatively extensive tendency toward dilation of sinusoid-like vascular spaces.

Pseudoglandular patterns are common morphological findings in well-to-moderately differentiated HCCs and are associated with a relatively hyperechogenic pattern. Several theories regarding their underlying mechanism have been proposed. Watanabe et al. revealed that hyperechogenicity on US is attributed to the reflection of US waves at the walls of numerous acini, as observed in hemangioma [28]. Edamitsu et al. reported that patients with pseudoglandular patterns in over one-third of their tumor lesions in the high-echoic group had a significantly larger mean pseudogland than the low-echoic or isoechoic group (123.4 ± 29.1 vs. 44.5 ± 5.2 μm) ($p < 0.02$) [29]. Results showed that the pseudogland diameter was a major factor in determining the echo level. Ishida et al. revealed that the hyperechogenicity of HCC with a pseudoglandular pattern was attributed to a pinkish substance similar to an amorphous hyaline in the dilated pseudoglands [30]. Further, they observed that the sizable pseudoglandular structures with colloid-like structures were high-echogenic lesions, and that they resembled thyroid follicles or cast deposition within the collecting tubules in newborn kidneys. Therefore, the extended and expanded lumen of the pseudogland and internal substances contribute to the echogenic level. Nonetheless, the involvement of amorphous materials in the mechanism that leads to the relatively hyperechogenic nature of the pseudoglandular pattern remains unclear. This lack of clarity persists even though the discussion by Ishida et al. has not been substantiated.

In Fig. 5, several lesions were hyperechogenic. However, a close histological examination revealed that only small areas had fatty deposits. Moreover, the lesion presented with pseudoglandular patterns in several areas.

Liver metastasis

Metastatic liver tumors are often accompanied by necrosis inside and outside the tumor nests (Fig. 6). In addition, they can be observed as partially hyperechoic based on the mode of distribution of the necrotic material. For example, the well-known bull's eye pattern is interpreted as limbal

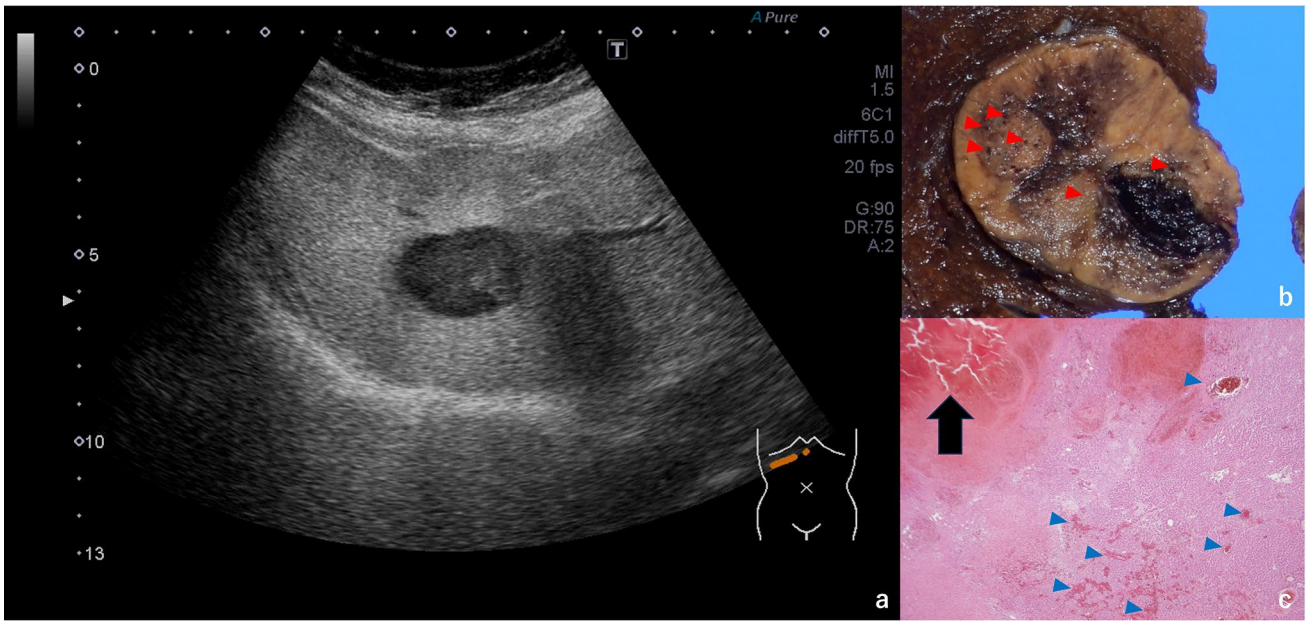

Fig. 3 Hepatocellular carcinoma with peliotic change. A liver mass was found, and most lesions appeared hyperechoic (**a**). Several black-speckled structures were observed within the lesion protruding into the split surface (red arrowhead) (**b**). Histological examination using hematoxylin and eosin staining revealed peliotic change with blood congestion in the sinusoidal-like lumen (blue arrowhead). In this case, some bleeding with clotting was also observed (black arrow); however, peliotic changes are often not accompanied by clotting (**c**)

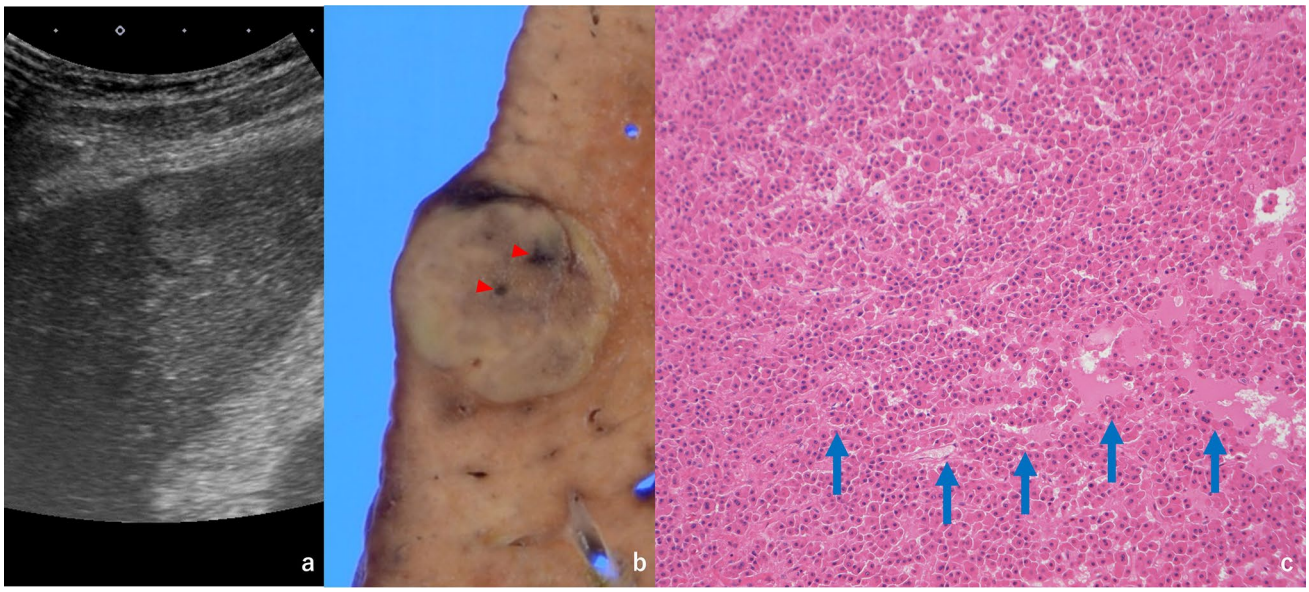

Fig. 4 Hepatocellular carcinoma. Most lesions appeared brighter on ultrasonography (**a**). Macroscopically, peliotic changes were limited to small areas (red arrowhead) (**b**). Histopathological examination showed dilated sinusoid-like vascular spaces between tumor cells (blue arrow) (**c**)

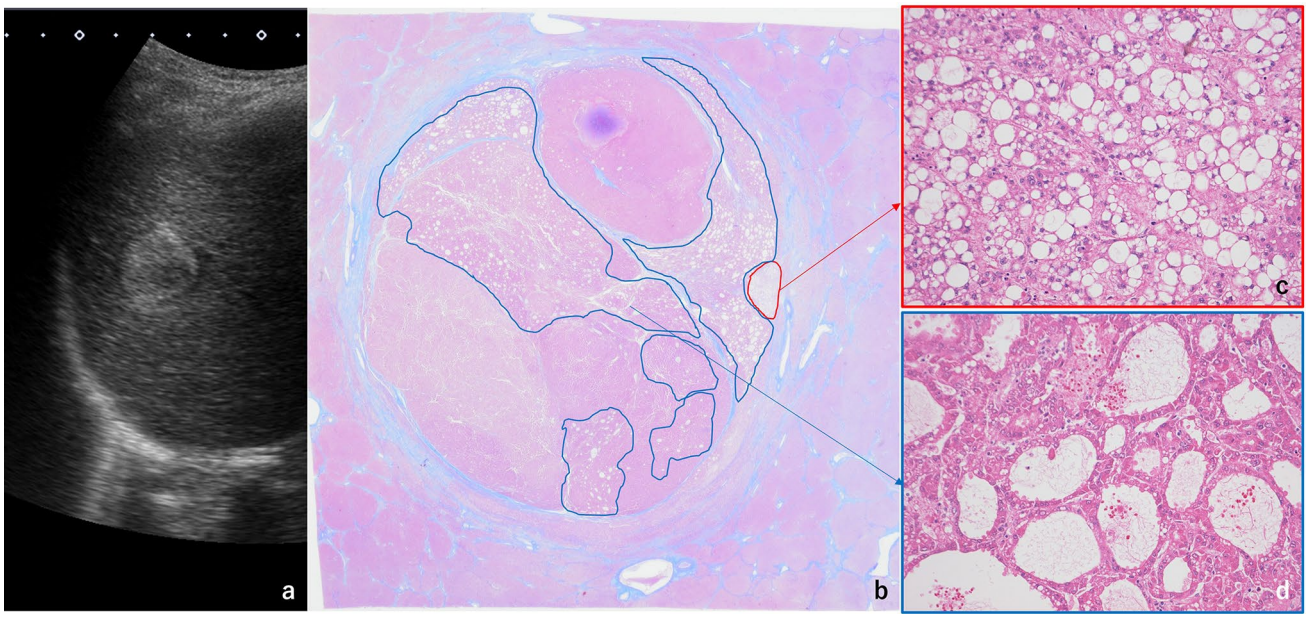

Fig. 5 Hepatocellular carcinoma. A hepatic mass had a high echogenicity on the major part of the lesion (**a**). Histological examination revealed fatty deposits only in the small area circled by the red line after staining with Azan (**b**) and hematoxylin and eosin (**c**). Pseudoglandular patterns were noted in the area circled by the blue line (b and d, hematoxylin and eosin stain)

hypoechogenicity and central hyperechogenicity caused by the presence of viable cancer cells at the limbus and necrosis in the center [9, 31, 32]. Notably, necrotic areas can appear as either hyperechoic or hypoechoic based on their histology.

Marked mucin production and comedo are associated with hyperechoic US images of metastatic adenocarcinoma [33]. The comedo pattern or comedo necrosis, referred to as intraglandular necrosis, is a well-known finding in human epidermal growth factor receptor 2-positive ductal carcinoma of the breast, and is a necrosis phenotype. Echogenic foci can indicate comedo necrosis and/or calcifications in breast cancer [34], similar to those in the

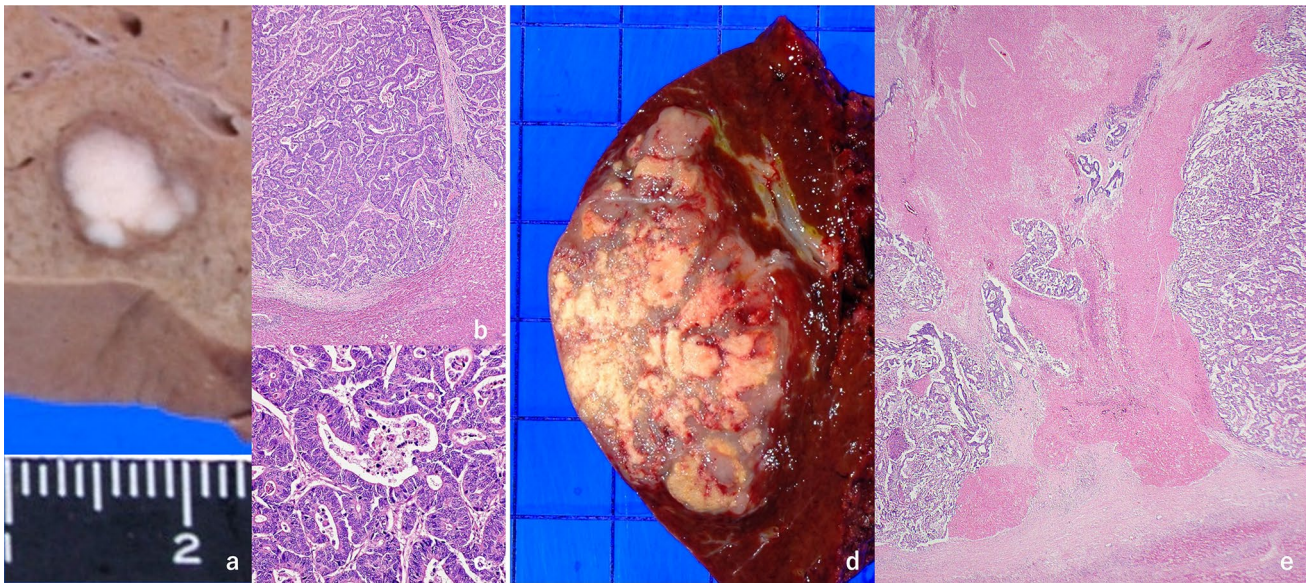

Fig. 6 Pathological features of liver metastasis from gastrointestinal cancer. In general, if the tumor size is small, necrosis is often not noticeable macroscopically (**a**). However, histological examination may show necrosis within the tumor lumen (**b**, **c**). By contrast, as the tumor size increases, necrosis is more likely to spread both inside and outside of the viable tumor cell nest (**d**, **e**)

liver. Moreover, some reports have shown that microcalcification is a major cause of intraluminal/intraglandular necrosis including comedo necrosis. However, cases of relative hyperechogenicity in the absence of calcification have been observed. However, there were areas of necrotic material in the tumor lumen (Fig. 7).

Neuroendocrine neoplasm

Primary hepatic neuroendocrine neoplasm (NEN) is a rare condition. Even if a solitary NEN is found in the liver, it is often considered as metastasis from other organs [35, 36]. NENs include well-differentiated neuroendocrine tumors (NETs), poorly differentiated neuroendocrine carcinomas

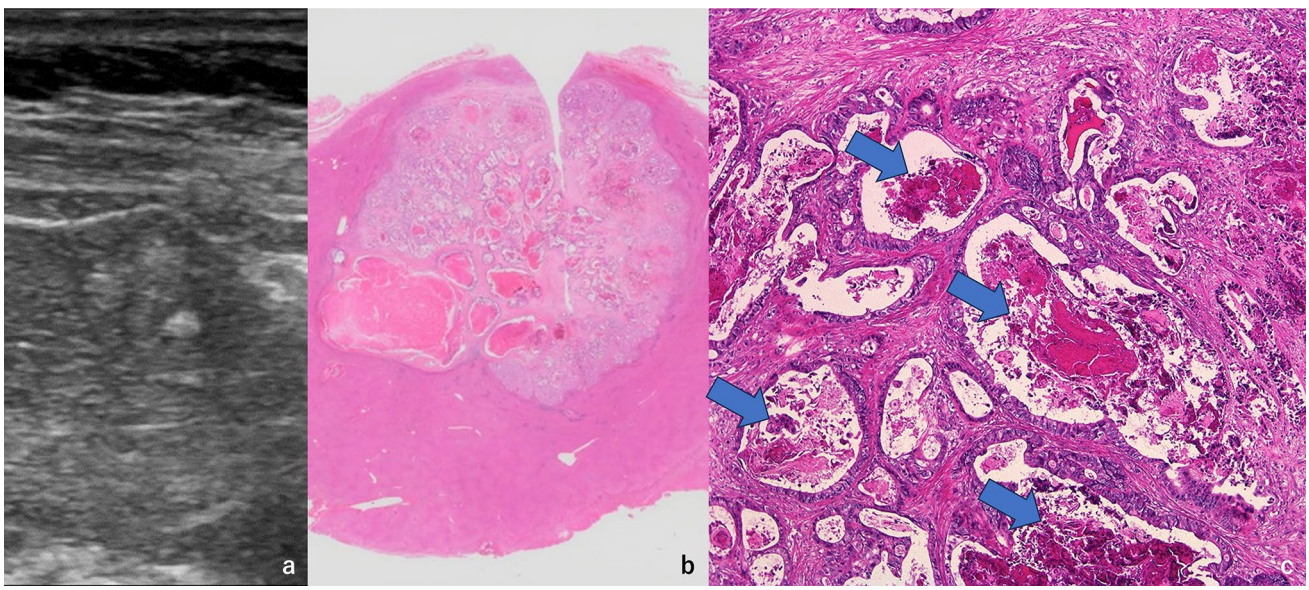

Fig. 7 Liver metastasis from sigmoid colon cancer. Ultrasonography revealed a lesion near the surface of the liver with multiple areas of high echogenicity (**a**). Histologically, comedo necrosis prominently appeared in the lumen (blue arrow) without calcification (**b**, **c**)

(NECs), and mixed neuroendocrine-non-neuroendocrine neoplasms [37].

In a previous study, 38.9% of patients with liver metastasis from NEN presented with hyperechogenicity on intraoperative US [38]. By contrast, hepatic metastases of NETs are often sporadically reported to be accompanied by cystic changes [39–41]. This change is often attributed to tumor cell degeneration or necrosis. However, in our cases, abundant blood cavities between NET cells often expanded to form blood lakes, and the mechanism may be different from cavity formation associated with necrosis of adenocarcinoma (Fig. 8). In addition, a detailed observation of our case showed that the solid area was more hyperechoic than the surrounding liver tissue, which may have been due to the relatively wide blood sinuses between tumor cells (sinusoidal-like vessel dilation).

NEC can appear in various organs and can be classified into large and small cell types in the digestive system, both of which show an aggressive behavior [42]. There are no comprehensive reports on the ultrasonographic findings of liver metastases from NEC. However, they are often clinically different from those of common adenocarcinomas. In our case involving a metastatic large cell NEC component from gastric mixed neuroendocrine-non-neuroendocrine neoplasms (Fig. 9), the growth pattern was a combination of fully expansive areas and abundant necrosis. The cellular architecture was a mixture of thick trabecular structures, thin cord-like structures, glandular/ductal structures, and rosette formation. The distance between the cell nuclei was heterogeneous, reflecting the irregularity in the size of the nuclei and the disorganization of the cordate architecture. These mixed patterns may have contributed to the relatively hyperechogenic, irregular bull's eye-like pattern. In this case, the tumor border was smoother than that in common metastases of gastrointestinal adenocarcinoma, probably reflecting a rapid expansive growth pattern.

Intrahepatic cholangiocarcinoma

Intrahepatic cholangiocarcinomas (iCCAs) generally have low echogenicity, or they occasionally have mixed echogenicity [9, 43]. A mass-forming iCCA is firm and whitish gray in color because it has a large amount of fibrous stroma and is often mixed with necrosis [44]. The level of echo in iCCA is affected by the combination of materials with different acoustic impedances, such as tumor glands, collagenous stroma, and necrotic components. However, some iCCAs may have a mix of hyperechogenic areas due to the presence of special histologic types within the tumor. Figure 10 shows two cases at our institution in which small-duct iCCAs were accompanied by ductal plate malformation (DPM)-like features [45]. DPM is a developmental anomaly resulting in the partial persistence of redundant embryonic bile duct structures, known as ductal plates [46]. iCCAs with DPM-like features are similar to DPM histopathologically. Tumor epithelial components are glandular structures with irregularly dilated lumens. The luminal part of the gland does not present with signs of necrosis or mucus accumulation. In our

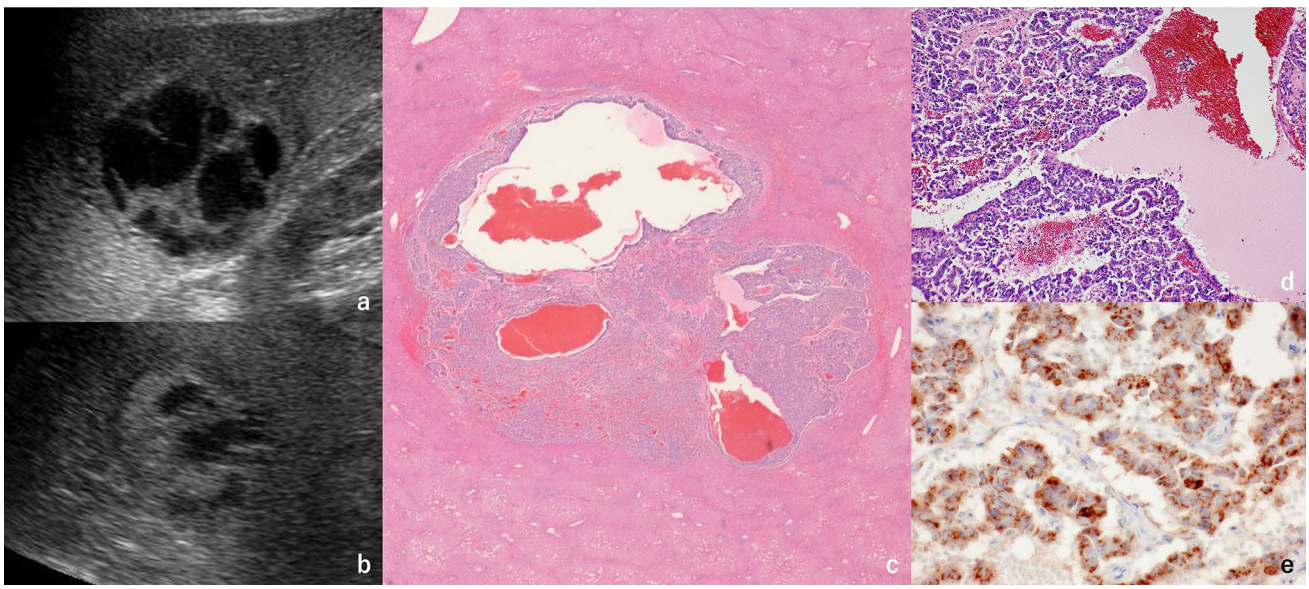

Fig. 8 Metastatic neuroendocrine tumor of the liver. Cystic changes were observed on ultrasonography (**a**, **b**) and hematoxylin and eosin stain (**c**). At a high-power view, blood sinuses were abundant between the cord-like proliferating tumor cells, which often dilate and store blood inside (**d**). Immunohistochemistry of chromogranin A clearly reveals the presence of tumor cells running in a cord-like pattern and dilated sinusoidal structures in the spaces between the cells (**e**)

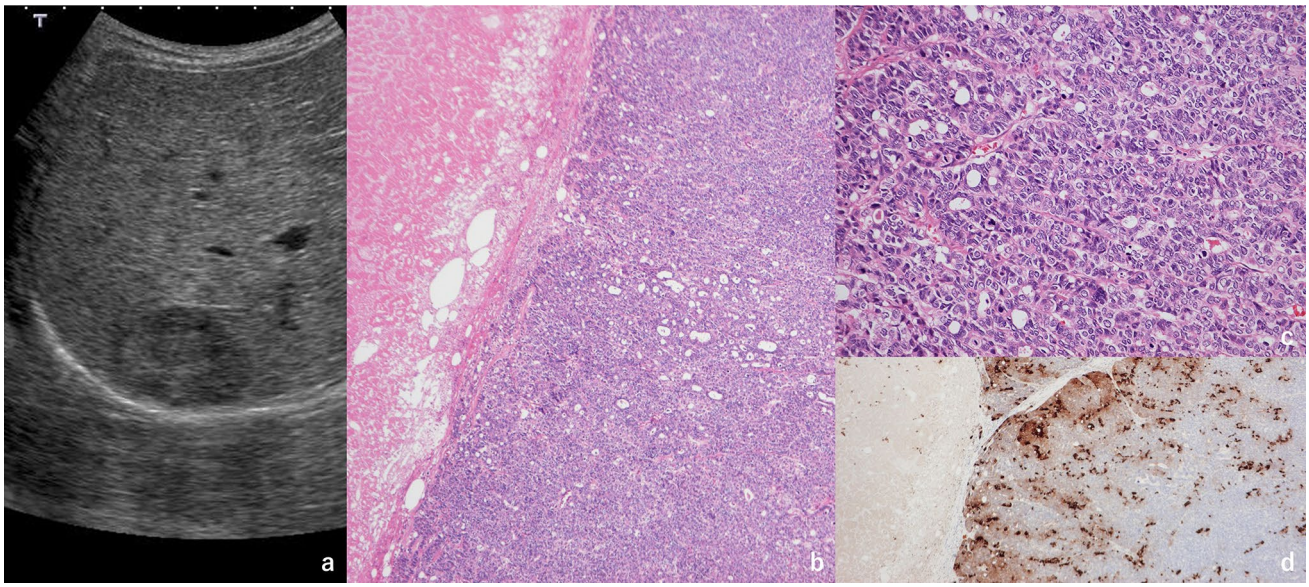

Fig. 9 Liver metastatic lesion of mixed neuroendocrine-non-neuroendocrine neoplasm from the stomach. Approximately half of gastric lesions are adenocarcinomas. Meanwhile, large cell neuroendocrine carcinoma components account for most liver metastatic lesions. On ultrasonography examination, irregular, highly echogenic areas were observed within the lesion (**a**). Histological examination revealed medium to large cancer cells with a high nuclear-to-cytoplasmic ratio appearing with irregular trabecular structures with necrosis (**b**, **c**). The tumor cells tested positive for chromogranin A (**d**)

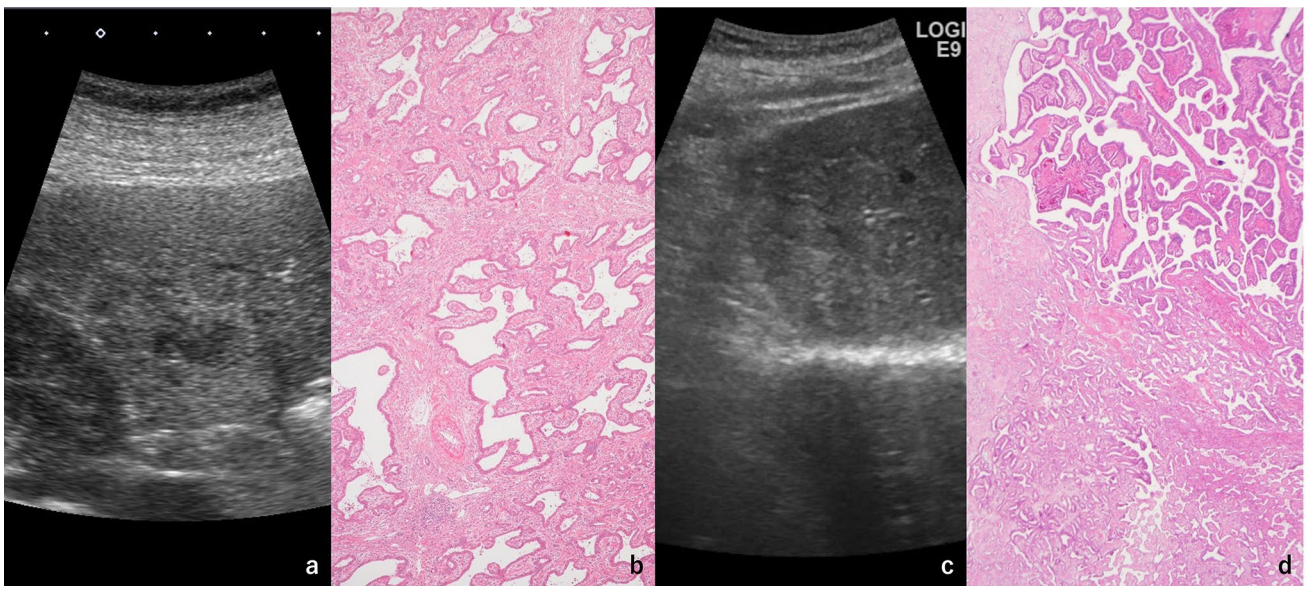

Fig. 10 Intrahepatic cholangiocarcinoma. Case 1: Ultrasonography revealed a lobulated nodular lesion with mostly hyperechoic areas (**a**). Histological examination showed a small duct-type intrahepatic cholangiocarcinoma with ductal plate malformation-like changes, including dilatation and anastomosis (**b**). Case 2: Ultrasonography showed a lobulated nodule with unclear borders and hyperechoic areas (**c**). Microscopic examination revealed that the lesion was an intrahepatic cholangiocarcinoma with focal ductal plate malformation-like changes. The tumor glands were significantly dilated and had anastomosis (**d**)

two cases, these areas appeared as hyperechogenic compared with the surrounding area. The dilated lumen of the gland had multiple bordering surfaces, which may have caused its relative hyperechogenicity.

Hemangioma

Based on previous studies, hemangiomas are the most commonly detected hyperechogenic lesions on liver US [10–13]. Approximately 70% of hemangiomas are hyperechogenic, and the remaining 30% are hypoechogenic or have mixed echogenicity [14].

The difference in the echo levels between hemangiomas is usually attributed to the vessel lumen size and the presence or absence of sclerosing changes (Fig. 11). The presence of multiple internal boundary surfaces and the combination of physical properties with different acoustic impedances, such as the vessel wall and blood component, may cause relative hyperechogenicity. The lumen of a hemangioma is filled with noncoagulated blood, and it typically lacks colloid-like substances.

In 1993, Moody et al. reported that an echogenic border was observed as a thick echogenic rind or a thin rim, which is a finding of hemangioma [47], and was later known as a marginal strong echo [48]. Histologically, some hemangiomas present with a distinct combination of blood vessels and background liver tissues at their margins (Fig. 11e and f) resembling a ria coast or fjord. These areas are believed to produce high echoes because of the combination of materials and different acoustic impedances.

Notably, the phenomenon of increased echo levels in localized lesions in the liver caused by the combination of materials with different acoustic impedances is only possible in relation to the surrounding tissues. For example, hemangioma in a normal liver is hyperechogenic; however, if the patient gains weight and has a fatty liver, the hemangioma presents as hypoechogenic.

Focal nodular hyperplasia

FNH is a noncancerous lesion that is believed to be a hyperplastic response of the liver parenchyma to the presence of a pre-existing vascular malformation [49]. In practice, the size and shape of the abnormal vessels in the center of the FNH vary from case to case. In some cases, they can be observed as a grossly visible star-shaped scar. Meanwhile, in others, they are merely fragile vascular growths that can only be identified on histological examination.

Figure 12 shows three different cases of FNH. The first case (Fig. 12a and b) involved a well-defined nodular lesion with hypoechogenic and partially isoechoic internal echogenicity. In this case, the spoke-wheel appearance was observed on color Doppler US (Fig. 12b). Notably, B-mode US of FNH is usually non-specific, and the detection of a

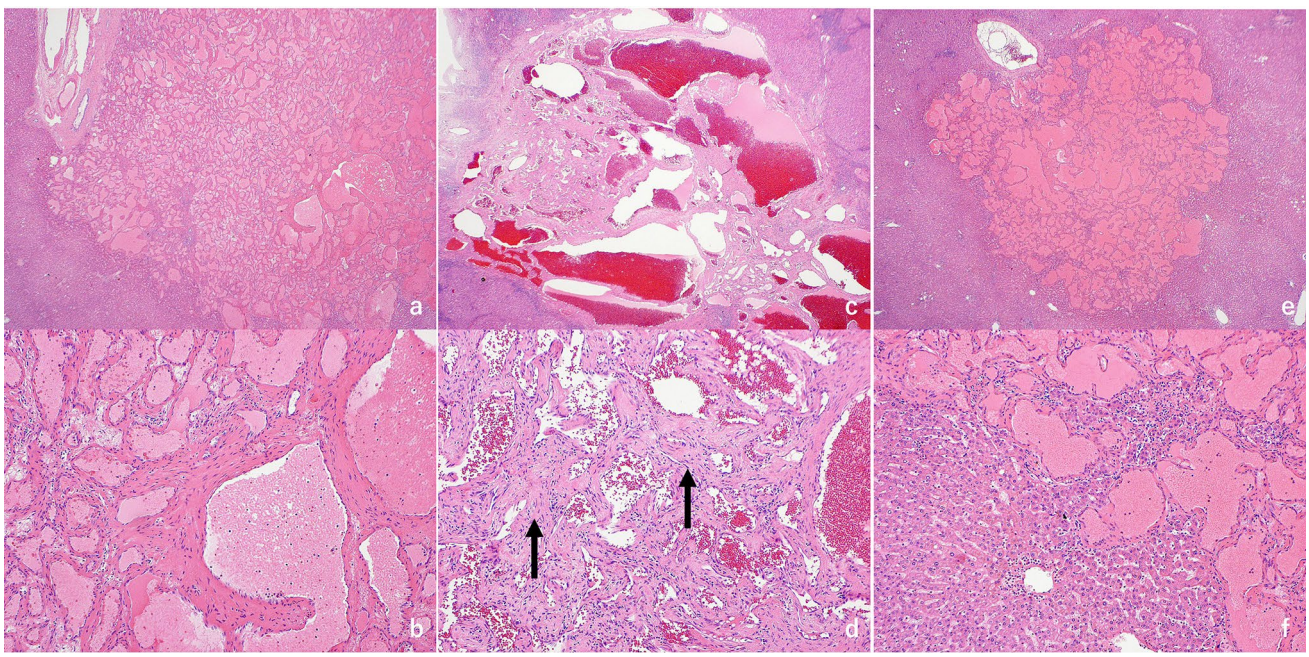

Fig. 11 Various hemangiomas. Case 1 (**a**, **b**): A 6-mm hemangioma, which is a benign tumor composed of blood vessels, was observed. A closer examination revealed several veins with different sizes and thicknesses. Case 2 (**c**, **d**): An 8-mm hemangioma was detected, and sclerosed changes were observed in some areas (black arrow). Case 3 (**e**, **f**): A 4-mm hemangioma was noted, and a mixture of vascular components and surrounding liver tissues were found at its margins, giving the appearance of a deeply indented coastline or fjord

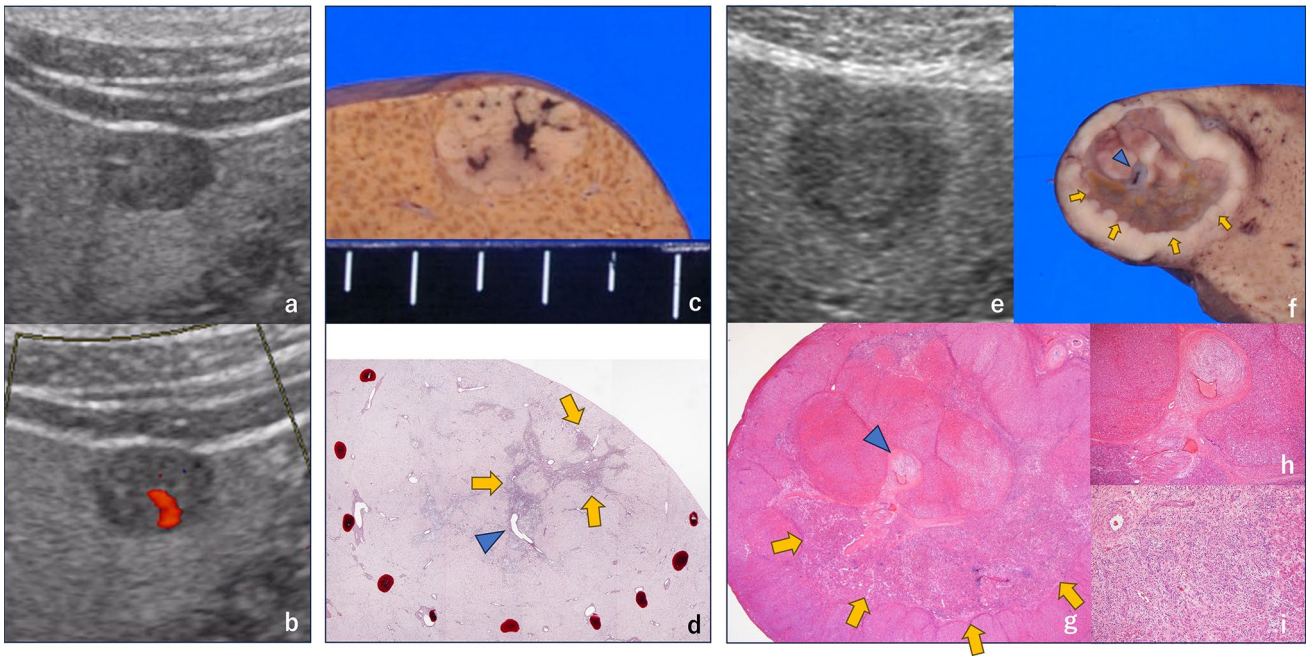

Fig. 12 Focal nodular hyperplasia (FNH). Case 1 (**a**, **b**): A well-defined nodular lesion with hypoechogenic and partially isoechoic internal echogenicity. The so-called spoke-wheel appearance was observed on color Doppler (**b**). Case 2 (**c**, **d**): A 10-mm FNH. Irregular vessels (blue arrowheads) and hepatocellular collapse (yellow arrow) were found on Gitter staining (**d**). Case 3 (**e–i**). FNH with a large central scar. A relative hyperechogenic area was clearly observed in the interior part (**e**). Irregular vessels (blue arrowheads) could be pointed out (**f–h**). A broad scar lesion with inflammation, hepatocellular collapse, ductular reaction, and capillary growth (yellow arrow, **f**, **g**, and **i**) were observed around the irregular artery

spoke-wheel appearance on color Doppler US is not often successful [15, 50]. The second case (Fig. 12c and d) involved a 10-mm FNH that was incidentally included in the surgical resection specimen for another malignancy. In this lesion, irregular vessels (blue arrowheads) and hepatocellular collapse (yellow arrow) were histologically evident, despite the stellate scar not being grossly visible. As shown in Fig. 12e–i, in the third case, a conclusive diagnosis of FNH was not established prior to surgery. Hepatocellular adenoma could not be excluded as a possibility, which led to the patient opting for resection. On US, a relatively hyperechogenic area was clearly observed in the interior (Fig. 12e). Macroscopic examination of the lesion revealed a light brownish color at the margins and a brownish-brown interior (Fig. 12f). Histologically, an abnormal artery was observed in the center of the lesion (Fig. 12g (blue arrowhead) and Fig. 12h), surrounded by a broad scar lesion with widespread inflammation, hepatocellular collapse, ductular reaction, and granulation-like capillary growth. The common feature among the three cases was arterial vessel malformation in the center. The size of the hyperechogenic lesion could vary based on the size, shape, and histological diversity of the so-called scar lesions that form around the abnormal vessels.

Angiomyolipoma

Angiomyolipoma (AML) is a neoplastic lesion of the liver containing various proportions of tortuous blood vessels, smooth muscle, and fat [51]. When diagnosing AML, the presence of mixed hyperechogenic areas can be misinterpreted as fat deposition without the help of contrast-enhanced MRI or pathological examination. However, the hyperechogenic regions that are observed within AML do not always contain fat.

Figure 13 shows a US image, MRI images, and histopathological image of AML. A well-defined, oval-shaped mass lesion measuring 40 mm presented with multiple internal geographical hyperechoic areas (Fig. 13a). On the T1-weighted MRI image, the out-of-phase signal area (red arrow) was reduced (Fig. 13b) compared with the in-phase area (Fig. 13c), thereby indicating fat deposition in the same area. Notably, the fat content region identified on MRI was significantly smaller than the high-echo region detected on US. Grossly and histologically, the lesions had various characteristics (Fig. 13d and e), i.e., sinusoidal dilation (Fig. 13f), tortuous arteries (Fig. 13g), fat deposition (Fig. 13h), and intercellular lymphocytic infiltration (Fig. 13i). AML of the liver often has a low fat content,

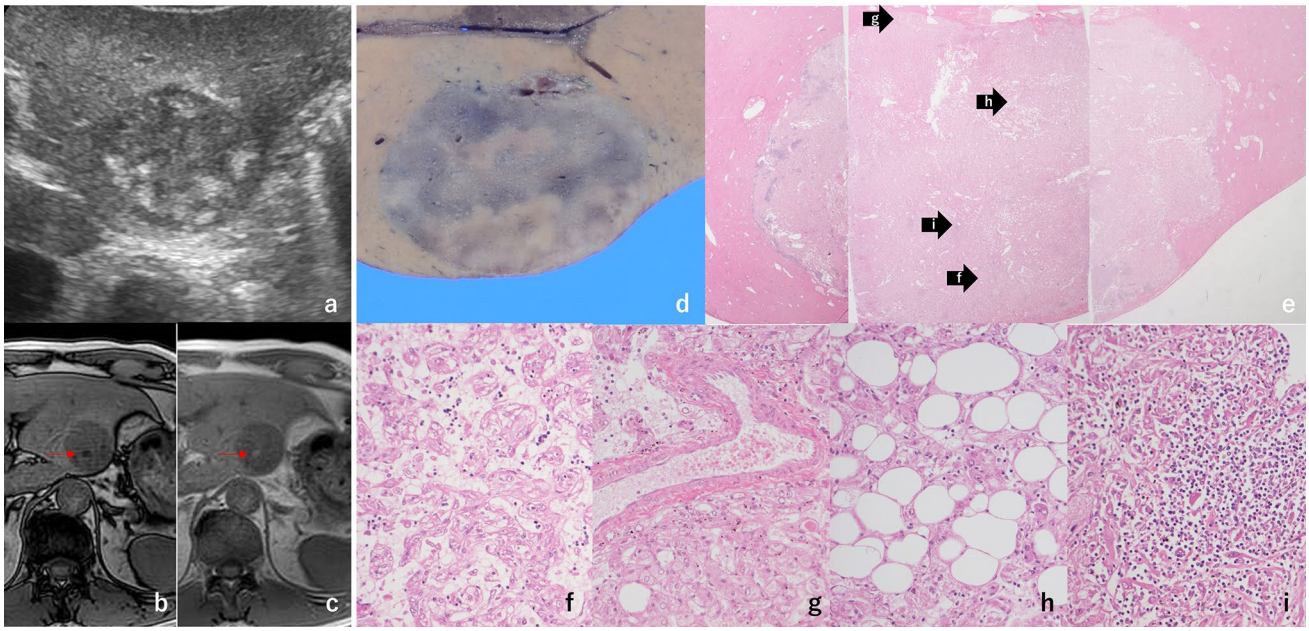

Fig. 13 Angiomyolipoma. A well-defined oval-shaped mass lesion measuring 40 mm with internal geographical hyperechoic areas (**a**). Out-of-phase (**b**) and in-phase (**c**) T1-weighted magnetic resonance imaging showed fat deposition (red arrow). Gross (**d**) and histological (**e**) examination revealed various characteristics. Sinusoidal dilation (**f**), tortuous arteries (**g**), fat deposition (**h**), and intercellular lymphocytic infiltration (**i**) could be observed

which is more difficult to diagnose preoperatively than lipomatous AML. Moreover, this lesion is challenging to differentiate from conditions such as HCC and hepatocellular adenoma [52]. In such a case, surgery is performed due to the risk of malignancy, which cannot be ruled out before surgery. Despite the small fat-containing area on MRI, the internal echoes of the lesion were significantly higher and more irregular than those of a normal HCC. This could have predicted the presence of sinusoidal dilation or other phenomena in the lesion before surgery.

Conclusion

Hyperechogenicity in hepatic lesions can be attributed to various reasons other than fatty deposits. The differences in echo levels observed in pathological findings can be caused by the degree of property mixing in a particular area. The histological nature of the lesion can result in different patterns of tissue mixing, which can lead to these discrepancies.

Declarations

Conflict of interest The authors declare no conflicts of interest.

Ethical statements All procedures were performed according to the ethical standards of the responsible committee on human experimentation (institutional and national) and the 1964 Declaration of Helsinki and its later versions.

References

1. Marrero JA, Ahn J, Rajender Reddy K, et al. ACG clinical guideline: the diagnosis and management of focal liver lesions. Am J Gastroenterol. 2014;109:1328–47.
2. Heimbach JK, Kulik LM, Finn RS, et al. AASLD guidelines for the treatment of hepatocellular carcinoma. Hepatology. 2018;67:358–80.
3. European Association for the Study of the Liver. Electronic address: easloffice@easloffice.eu, European Association for the study of the liver. EASL Clinical Practice guidelines: management of hepatocellular carcinoma. J Hepatol. 2018;69:182–236.
4. Marrero JA, Kulik LM, Sirlin CB, et al. Diagnosis, staging, and management of hepatocellular carcinoma: 2018 practice guidance by the American Association for the study of Liver diseases. Hepatology. 2018;68:723–50.
5. Minami Y, Nishida N, Kudo M. Imaging diagnosis of various hepatocellular carcinoma subtypes and its hypervascular mimics: differential diagnosis based on conventional interpretation and artificial intelligence. Liver Cancer. 2023;12:103–15.
6. Matos AP, Velloni F, Ramalho M, et al. Focal liver lesions: practical magnetic resonance imaging approach. World J Hepatol. 2015;7:1987–2008.
7. Harvey CJ, Albrecht T. Ultrasound of focal liver lesions. Eur Radiol. 2001;11:1578–93.
8. Schwerk WB, Schmitz-Moormann P. Ultrasonically guided fine-needle biopsies in neoplastic liver disease: cytohistologic diagnoses and echo pattern of lesions. Cancer. 1981;48:1469–77.

9. Minami Y, Kudo M. Hepatic malignancies: correlation between sonographic findings and pathological features. World J Radiol. 2010;2:249–56.
10. Bree RL, Schwab RE, Neiman HL. Solitary echogenic spot in the liver: is it diagnostic of a hemangioma? AJR Am J Roentgenol. 1983;140:41–5.
11. Gibney RG, Hendin AP, Cooperberg PL. Sonographically detected hepatic hemangiomas: absence of change over time. AJR Am J Roentgenol. 1987;149:953–7.
12. Kimura Y, Fukada R, Katagiri S, et al. Evaluation of hyperechoic liver tumors in MHTS. J Med Syst. 1993;17:127–32.
13. Taboury J, Porcel A, Tubiana JM, et al. Cavernous hemangiomas of the liver studied by ultrasound. Enhancement posterior to a hyperechoic mass as a sign of hypervascularity. Radiology. 1983;149:781–5.
14. Nelson RC, Chezmar JL. Diagnostic approach to hepatic hemangiomas. Radiology. 1990;176:11–3.
15. Naganuma H, Ishida H, Ogawa M, et al. Focal nodular hyperplasia: our experience of 53 Japanese cases. J Med Ultrason. 2017;44:79–88.
16. Tanaka S, Kitamura T, Imaoka S, et al. Hepatocellular carcinoma: sonographic and histologic correlation. AJR Am J Roentgenol. 1983;140:701–7.
17. Tanaka H. Current role of ultrasound in the diagnosis of hepatocellular carcinoma. J Med Ultrason. 2020;47:239–55.
18. Oikawa T, Ojima H, Yamasaki S, et al. Multistep and multicentric development of hepatocellular carcinoma: histological analysis of 980 resected nodules. J Hepatol. 2005;42:225–9.
19. Seo J, Jeong DW, Park JW, et al. Fatty-acid-induced FABP5/HIF-1 reprograms lipid metabolism and enhances the proliferation of liver cancer cells. Commun Biol. 2020;3:638. https://doi.org/10.1038/s42003-020-01367-5.
20. Hayashi M, Matsui O, Ueda K, et al. Progression to hypervascular hepatocellular carcinoma: correlation with intranodular blood supply evaluated with CT during intraarterial injection of contrast material. Radiology. 2002;225:143–9.
21. Kojiro M. Nodule-in-nodule' appearance in hepatocellular carcinoma: its significance as a morphologic marker of dedifferentiation. Intervirology. 2004;47:179–83.
22. Ogata R, Majima Y, Tateishi Y, et al. Bright loop appearance; a characteristic ultrasonography sign of early hepatocellular carcinoma. Oncol Rep. 2000;7:1293–8.
23. Fujimoto M, Nakashima O, Komuta M, et al. Clinicopathological study of hepatocellular carcinoma with peliotic change. Oncol Lett. 2010;1:17–21.
24. Poisson J, Lemoinne S, Boulanger C, et al. Liver sinusoidal endothelial cells: physiology and role in liver diseases. J Hepatol. 2017;66:212–27.
25. Sugimachi K, Tanaka S, Taguchi K, et al. Angiopoietin switching regulates angiogenesis and progression of human hepatocellular carcinoma. J Clin Pathol. 2003;56:854–60.
26. Dong Y, Wang WP, Lim A, et al. Ultrasound findings in peliosis hepatis. Ultrasonography. 2021;40:546–54.
27. Hoshimoto S, Morise Z, Suzuki K, et al. Hepatocellular carcinoma with extensive peliotic change. J Hepatobil Pancreat Surg. 2009;16:566–70.
28. Watanabe H, Asayama Y, Nishie A, et al. A case of pseudoglandular hepatocellular carcinoma: the usefulness of a multimodal approach. Radiol Case Rep. 2018;13:689–92.
29. Edamitsu O, Kiyomatsu K, Nakashima O, et al. Pathomorphologic study on hepatocellular carcinoma showing hyperechoic pattern. Kanzo. 1991;32:618–24.
30. Ishida Y, Nagamatsu H, Koga H, et al. Hepatocellular carcinoma with a nodule-in-nodule appearance reflecting an unusual dilated pseudoglandular structure. Intern Med. 2008;47:1215–8.
31. Yoshida T, Matsue H, Okazaki N, et al. Ultrasonographic differentiation of hepatocellular carcinoma from metastatic liver cancer. J Clin Ultrasound. 1987;15:431–7.
32. Choti MA, Kaloma F, De Oliveira ML, et al. Patient variability in intraoperative ultrasonographic characteristics of colorectal liver metastases. Arch Surg. 2008;143:29–34. discussion 35.
33. Inoue T, Shiga J, Machinami R. Direct correlation between sonography and histology of minute malignant hepatic nodule. Pathol Res Pract. 1992;188:330–9.
34. Watanabe T, Yamaguchi T, Tsunoda H, et al. Ultrasound image classification of ductal carcinoma in situ (DCIS) of the breast: analysis of 705 DCIS lesions. Ultrasound Med Biol. 2017;43:918–25.
35. Nomura Y, Nakashima O, Akiba J, et al. Clinicopathological features of neoplasms with neuroendocrine differentiation occurring in the liver. J Clin Pathol. 2017;70:563–70.
36. Fenoglio LM, Severini S, Ferrigno D, et al. Primary hepatic carcinoid: a case report and literature review. World J Gastroenterol. 2009;15:2418–22.
37. Klimstra D. Hepatic neuroendocrine neoplasms. In: World Health Organ Classif Tumours Editorial Board, editor. WHO classification of tumours, Digestive tumours. Lyon (France). International Agency for Research on Cancer (IARC); 2019. p. 263–4.
38. Dogeas E, Chong CCN, Weiss MJ, et al. Can echogenic appearance of neuroendocrine liver metastases on intraoperative ultrasonography predict tumor biology and prognosis? HPB (Oxford). 2018;20:237–43.
39. Fiori S, Del Gobbo A, Gaudioso G, et al. Hepatic pseudocystic metastasis of well-differentiated ileal neuroendocrine tumor: a case report with review of the literature. Diagn Pathol. 2013;8:148.
40. Li H, El Jabbour TE, Nigam A, et al. Metastatic insulinoma presenting as a liver cyst. J Pathol Transl Med. 2019;53:148–51.
41. Morikawa K, Igarashi T, Misumi S, et al. A case of pseudocystic liver metastases from an atypical lung carcinoid tumor. Radiol Case Rep. 2019;14:595–601.
42. Klimstra DS, Klöppel G, La Rosa S, et al. Classification of neuroendocrine neoplasms of the digestive system. In: WHO, et al., editors. WHO Classification of tumours. Digestive system tumours. Lyon (France). Int Agency Res Cancer 2019. p. 16–9.
43. Colli A, Cocciolo M, Mumoli N, et al. Peripheral intrahepatic cholangiocarcinoma: ultrasound findings and differential diagnosis from hepatocellular carcinoma. Eur J Ultrasound. 1998;7:93–9.
44. Lim JH. Cholangiocarcinoma: morphologic classification according to growth pattern and imaging findings. AJR. 2003;181:819–27.
45. Nakanuma Y, Sripa B, Vatanasapt V, et al. Intrahepatic cholangiocarcinoma. WHO classification of tumours. Digestive system tumours. Lyon (France). International Agency for Research on Cancer; 2019. pp. 254–9.
46. Chung T, Rhee H, Shim HS, et al. Genetic, clinicopathological, and radiological features of intrahepatic cholangiocarcinoma with ductal plate malformation pattern. Gut Liver. 2022;16:613–24.
47. Moody AR, Wilson SR. Atypical hepatic hemangioma: a suggestive sonographic morphology. Radiology. 1993;188:413–7.
48. Terminology and Diagnostic Criteria Committee. Ultrasound diagnostic criteria for hepatic tumors. J Med Ultrason. 2014;41:113–23.
49. Wanless IR, Mawdsley C, Adams R. On the pathogenesis of focal nodular hyperplasia of the liver. Hepatology. 1985;5:1194–200.
50. Li W, Wang W, Liu G-J, et al. Differentiation of atypical hepatocellular carcinoma from focal nodular hyperplasia: diagnostic performance of contrast-enhanced US and microflow imaging. Radiology. 2015;275:870–9.
51. Goodman ZD, Ishak KG. Angiomyolipomas of the liver. Am J Surg Pathol. 1984;8:745–50.

52. Woo YM, Ryu SH, Min JW, et al. Angiomyolipoma of the liver without a fat component, mimicking a hepatocellular carcinoma. Korean J Gastroenterol. 2018;71:49–53.